Rare Event Simulations Reveal Subtle Key Steps in Aqueous Silicate Condensation

Mahmoud Moqadam, Enrico Riccardi, Thuat T. Trinh, Anders Lervik and Titus S. van Erp[a]

A replica exchange transition interface sampling (RETIS) study combined with Born-Oppenheimer molecular dynamics (BOMD) is used to investigate the dynamics, thermodynamics and mechanism of the early stages of the silicate condensation process. In this process, two silicate monomers, of which one anion species, form a negatively charged five-coordinated silicate dimer. In a second stage, this dimer can fall apart again, forming the original monomers, or release a water molecule into the solution. We studied the association and dissociation reaction in the gas phase, and the dissociation and water removal step in the aqueous phase. The results on the aqueous phase dissociation suggest two possible mechanisms. The breakage of the bond between the intermediate oxygen and the five-coordinated silicon is sometimes accompanied with a proton transfer. After the dissociation into silicate monomers, the anionic monomer is either the previously four-coordinated silicon or the previously five-coordinated silicon depending on whether the hydrogen transfer occurs or not. Our results show that the mechanism with proton transfer is highly predominant. The water removal simulations also show two possible mechanisms distinguished by the proton transfer reaction path. The proton transfer can either occur via a direct or via a water mediated reaction step. The calculations reveal that although both mechanisms contribute to the water removal process, the direct proton transfer is slightly favorable and occurs roughly in six out of ten occasions.

1 Introduction

The silicate condensation reaction is the basic step in the sol-gel chemistry and zeolite synthesis. Therefore, understanding the earlier stages of silicate oligomerization is of fundamental scientific and technological importance. The formation of the silicate dimer from two silicate monomers, a neutral and an anionic species, basically consists of two steps. The first step in this process is formation of the SiO−Si linkage between the reactants to form a five-coordinated silicate complex. This is an essential intermediate stage in the oligomerization reaction. In the second step, a water molecule is released from the silicate complex forming the silicate dimer (see Figure 1). The mechanism of silicate based reactions have been subject of intensive research during last decades, both experimentally [1–5] and theoretically. [6–17]

Several of the previous theoretical studies have concentrated on the energetics of cluster models either based on Hartree-Fock, [11,14,15,18,19] MP2, [11,14,15,19] or density functional theory (DFT) [6–8,10,13,20–23] in which the clusters are either described in

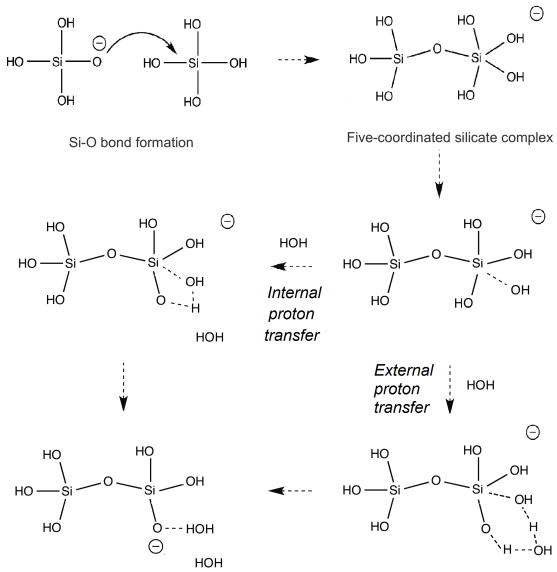

Fig. 1 The anionic mechanism of the silicate condensation reactions. The first step is formation of a five-coordinated silicate complex. Then, a water molecule dissociates from silicate complex either by an internal or external proton transfer and forms the silicate dimer.

[a] *Department of Chemistry, Norwegian University of Science and Technology (NTNU), Hgskoleringen 5, Realfagbygget D3-117 7491 Trondheim, Norway; Tel: +47 735 94142; E-mail: titus.van.erp@ntnu.no*

the gas phase or in a solvent using continuum solvent models. In particular, Pereira et al.[6–8] studied the silicate clusters using DFT coupled with the continuum solvation model COSMO (Conductor-like Screening MO method) to mimic the electrostatic conditions found in real silica solutions. Similarly, Xiao and Lasaga addressed the catalytic effect of OH^- in promoting the dissolution process in basic pH solutions.[19] The limited size of the silicate clusters allowed relatively high-level quantum chemical computations. In addition to energy barriers, reaction rates can be approximated using transition state theory.[11,14] However, these barriers and rates are not necessarily representable for the actual reactions in a solvent. Especially for water it is known that the solvent actively directs chemical reactions via its hydrogen bond network or participates in the reaction by accepting or donating protons.

The thermodynamic properties of silicate oligomerization process in explicit water have also been studied using Ab Initio molecular dynamics.[10,13,16] Since the accessible timescale of Ab Initio molecular dynamics is on the order of several picoseconds while the expectation time for a chemical reaction is many orders of magnitude larger, straightforward Ab Initio molecular dynamics is generally not useful to study chemical reactions. Still, thermodynamic quantities like the reaction free energy barriers and equilibrium constants can be obtained using standard constrained molecular dynamics methods and thermodynamic integration.[10,13,16,21–23]

Thermodynamic integration via constraint molecular dynamics[24] implies running several molecular dynamics simulations in which a predefined reaction coordinate (RC) is kept fixed by an artificial constraining force. Although it allows obtaining thermodynamic properties, information on the spontaneous dynamics is lost. An alternative approach is the use of classical molecular dynamics simulations based on reactive forcefields.[25–32] At this point, reactive force fields do not reach the same accuracy as DFT and might not always reliable,[16] but the accessible timescale of molecular dynamics with reactive forcefields is in the range of several nanoseconds. Therefore, it is able to capture the spontaneous reactive events in a wide range of chemical systems. Still, these studies often require temperatures far above experimental conditions to increase the frequency of reactive events.

Even faster than classical molecular dynamics is kinetic Monte Carlo (kMC)[33] which has been applied to investigate silicate oligomerization reactions.[34–36] The kinetic Monte Carlo typically requires as an input the diffusion constants of the reactants and rate constants of several elementary reaction steps. Zhang et al. developed a continuum off-lattice kMC model for the initial stage of silicate oligomerization based on rate constants from transition state theory from DFT calculations with explicit water molecules.[35] This method allows exploring initial stage of silicate oligomerization and the effect of pH at experimental conditions. More recently, a lattice-based kinetic Monte Carlo model was introduced by Ciantar et al.[36] to study the effect of molecular diffusion, synthesis parameters and initial monomer concentration on the steady state concentrations of silicate oligomers at the earlier stages of zeolite synthesis. This model allows automatic allocation of each species with a flexible use of various lattice types. The accessible timescale of kinetic Monte Carlo is enormous (minutes, hours) but its accuracy highly depends on the accuracy of the rate constants of the elementary steps which need to be provided as an input. In addition, detailed information about the actual reaction mechanism is lost.

Clearly, the above review shows that the computational study of the actual unbiased dynamics of the oligomerization process is still a huge challenge. Ideally, we would like to use accurate forces based on Ab Initio methods and still reach large timescales. Kinetic Monte Carlo has limited accuracy as mentioned above. ReaxFF increases the timescale compared to Ab Initio based molecular dynamics, but generally not enough to study the reactions at ambient condition. In addition, it requires choosing a parameter set or developing a new purpose-specific parameter set since we showed that simulations based on present ReaxFF forcefields[37,38] can produce unphysical reactions.[16]

An alternative approach which can be used in combination with any type of molecular dynamics is path sampling.[39–41] Path sampling allows the harvesting of statistically relevant ensembles of unbiased dynamical trajectories based on a combined Monte Carlo/molecular dynamics approach. Based on the ensemble conditions, these sets of paths will describe different stages of the reaction process. For instance, one ensemble condition could be that all path should start from the reactant state and end in the product state. Hence, this path ensemble only consists of reactive paths. Other path ensembles might only require the paths to reach a certain threshold point at the barrier. Path sampling allows overcoming high free energy barriers without artificially constraining the system or by applying an additional biasing force. Hence, it will provide the real dynamics of the process and, by combining the results of the different path ensembles, it can provide rate constants orders of magnitude faster than straightforward molecular dynamics. The efficiency of the original transition path sampling method[39] was consecutively improved by the TIS[40] and RETIS[41] algorithms and has now matured as a powerful method to study unbiased reactive events. In this article, we will use RETIS in combination with Ab Initio molecular dynamics, which has not been used before, in order to shed light on yet unresolved questions regarding the spontaneous oligomeriztion process.

For example, Pavlova et al.[13] reported that the water removal step of silicate dimerization and trimerization reaction occurs through the external proton transfer mechanism, while Trinh et al.[10] denoted that in the dimerization reaction only the internal proton transfer mechanism occurs. In some cases, they observed the external proton transfer mechanism in the trimerization reaction. In contrast, McIntosh detected both internal and external mechanisms in the silicate dimerization reactions.[11] However, the author concluded that internal mechanism is highly favorable compared to the external mechanism. Based on the available literature it is difficult to state a final conclusion since the aforementioned studies all depend on different level of assumptions and approximations or steer the reaction in an artificial manner. RETIS with Ab Initio molecular dynamics is, therefore, a very valuable complementary method to the studies above as it is the only method that can provide the correct statistics of un-

biased dynamical reactive trajectories in explicit water based on state-of-the-art DFT level energies and forces.

Path sampling with Ab Initio molecular dynamics has been used before for the study of water autoionization,[42] fenton reactions,[43] gas-phase decomposition reactions,[44] and enzyme catalysis.[45] However, these papers are based on the original TPS[39] algorithm employing a single path ensemble of reactive trajectories. This study is the first one where the RETIS methodology is applied in combination with Ab Initio dynamics using many different path ensembles. Hence, it is the first really quantitative Ab Initio path sampling study which allows the calculation of rates, crossing probabilities, and activation energies.

This article is organized as follows. In Section 2 we give an explanation of the RETIS methodology used in the work. In Section 3 we give the computational details for our approach. In Section 4 we provide the results accompanied with discussion for the gas-phase dissociation and association reaction, and the aqueous phase dissociation and water removal step. We end with concluding remarks in Section 5.

2 Methodology

The typical reaction times of the chemical reaction steps in the dimerization process are generally beyond the accessible timescale of molecular dynamics. Hence, it is extremely unlikely to detect any of such rare events in a direct simulation. Still, these events can be captured via the RETIS algorithm,[41] which can be combined with any type of dynamics such as classical MD, Langevin, or Ab Initio MD. Whereas the first Ab Initio MD simulations were based on the Car-Parrinello approach,[46] which launched the sudden popularity of these type of simulations, the advance in speed of electronic groundstate optimization algorithms have made BOMD the method of choice for Ab Initio MD. In this article, the RETIS algorithm has been combined with the BOMD utility of the CP2K[47] Quickstep routine.

RETIS is a path sampling method based on transition path sampling techniques (TPS)[39] allowing for an efficient quantitative analysis of chemical reaction and rare events in general. TPS has pioneered the idea to use Monte Carlo (MC) to sample short molecular dynamics reactive trajectories. In this way, the approach allows us to focus on those segments of the time evolution where the rare events actually occur. The original TPS publication[39] also provided a strategy to use this approach for calculating rate constants though not in the most efficient way. The TIS algorithm[40] improved the efficiency by a factor five for a simple two-state dimer molecule imersed in a solvent by allowing flexible path lengths and the introduction of interface path ensemble averages. The efficiency was further improved in the RETIS algorithm[41] by applying replica exchange between the different path ensembles. This approach showed a factor 20 improvement compared to TIS when studying the denaturation of a mesoscopic DNA model.[48] Although it is difficult to make a statement about the relative algorithmic efficiency in general, one can prove that the efficiency always increases when going from the original TPS algorithm to TIS and from TIS to RETIS. Based on the numbers above, the RETIS approach can easily account for a two orders of magnitude overall improvement compared to the original TPS algorithm. It is important to note that is improvement is achieved without invoking any approximation. On the contrary, the TIS/RETIS approach is also slightly more accurate since they are not restricted to a fixed path length; the average path length in TIS/RETIS is reduced compared to TPS but occasionally longer than the typical fixed path length used in TPS simulations.

The TIS/RETIS algorithm introduces a set of interfaces between the reactant and the product state and computes the overall crossing probability as a product of crossing probabilities for the intermediate interfaces. The TIS equations for transition between two stable states are:

$$k_{AB} = f_A \, \mathscr{P}_A(\lambda_B|\lambda_A) \tag{1}$$

$$\mathscr{P}_A(\lambda_B|\lambda_A) = \mathscr{P}_A(\lambda_n|\lambda_0) = \prod_{i=0}^{n-1} \mathscr{P}_A(\lambda_{i+1}|\lambda_i) \tag{2}$$

where f_A is the flux through the first interface λ_0. The flux term is determined in the RETIS algorithm from the average path lengths in the first two path ensembles, called $[0^-]$ and $[0^+]$.[41] These path ensembles have as only condition that they should start at the first interface $\lambda_0 = \lambda_A$ and from there move towards the reactant state ($[0^-]$) or towards the product state ($[0^+]$). These paths are ended when they recross λ_A or $\lambda_B = \lambda_n$. The latter is only possible for the $[0^+]$ ensemble, but unlikely since it is a rare event. The chance that this happens is equal to $\mathscr{P}_A(\lambda_B|\lambda_A)$ which is called the overall crossing probability. This is the probability that whenever the system crosses λ_A, it will cross λ_B before it crosses λ_A again. As λ_B is positioned a surface at the other side of the barrier, this probability is very small and can not be calculated directly. However, in TIS/RETIS it is determined by a series of path sampling simulations using the factorization given in equation (2). Here, $\mathscr{P}_A(\lambda_{i+1}|\lambda_i)$ is the conditional crossing probability that λ_{i+1} will be crossed before λ_A under the condition that the trajectory starting from λ_A has also crossed λ_i. Determination of this term requires the sampling of the $[i^+]$ path ensemble which contain all possible trajectories starting at λ_A, ending at λ_A or λ_B, and having at least one crossing with interface λ_i in between. This sampling can be done efficiently via MC moves in trajectory space such as shooting and time-reversal moves, which were developed within the TPS framework.[49] In RETIS this is completed with replica exchange moves. $\mathscr{P}_A(\lambda_{i+1}|\lambda_i)$ is finally estimated from the fraction of trajectories in the $[i^+]$ ensemble that cross λ_{i+1} as well. It should be noted that the overall reaction rate does not depend on the positions or the number of the interfaces, however, efficiency does. If the crossing probabilities are all around 0.2 the simulation set up is considered to be close to optimum.[50]

As reaction coordinate we chose the Si−O distance of the bond that will be created or broken in the dissociation and association reaction. In the water removal step, the reaction coordinate is MAX[Si−OH] which implies that the value of the reaction coordinate corresponds to the largest Si−OH distance in the five-coordinated silicon. This approach guarantees that the leaving OH group can be any Si−OH bond of the five-coordinated silicon (see Figure 2).

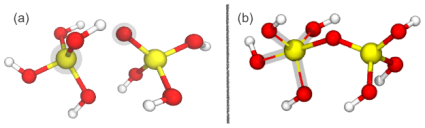

Fig. 2 Illustration of the reaction coordinate used in the RETIS simulation. Highlighted atoms and bonds show the atoms and bonds related to the reaction coordinate. (a) Formation and dissociation of silicate complex. The reaction coordinate is defines as Si−O distance, the distance between the five-coordinated silicon and the bridging or the anion oxygen. (b) Water removal step. The reaction coordinate is MAX[Si−OH] which is the maximum distance between oxygen and the five-coordinated silicon.

Besides reaction rates, path sampling also allows determining the activation energy of the reaction.[51] In the case of deterministic dynamics, the activation energy is equivalent to the difference between the average energy of state A and the average energy of the transition pathways connecting state A with state B.[51] Consequently, the calculation of activation energy barrier does not require all interface ensembles. However, if all the path ensembles are available, like in a TIS or RETIS simulation, an activation energy profile as function of the reaction coordinate can be obtained.[50] Analogous to the crossing probability, the function converges to a plateau value equal to the activation energy of the reaction. The function is expected to be strictly increasing, but not necessarily. Dips or sudden changes in slope of the activation energy function might indicate a complex reaction step at the value of the reaction coordinate where it happens. The total energy of the system is an extensive variable. Hence, it increases if, for instance, more solvent molecules are added to the system. However, the activation energy is an intensive variable. This implies that for large systems this activation energy is a relative small energy difference between two ensemble average which have much larger standard deviation than this difference. Therefore, accurate evaluation of the activation energy becomes problematic for the larger systems.

3 Computational Details

We studied the formation of five-coordinated silicate complex from one silicic acid $Si(OH)_4$ and its deprotonated form $Si(OH)_3O^-$ in gas and aqueous phase by coupling the RETIS algorithm with the DFT-based molecular dynamics simulation package Quickstep of the CP2K code.[47,52] The CP2K part of the simulation scheme employed the BLYP functional with Grimme's empirical dispersion correction[53–56] and Goedecker-Teter-Hutter (GTH) pseudopotentials.[57,58] The BLYP functional has shown to give an accurate description of the structure and dynamics of water and of the silica-water interaction.[10,16,59,60] A Gaussian basis set DZVP-MOLOPT[61] was chosen in addition to a plane-wave basis set with a cutoff of cutoff 400 Ry. In the gas phase, the simulations were performed using a cubic simulation box of $13\times13\times13$ Å^3 with periodic boundaries containing $Si(OH)_4$ and its deprotonated form $Si(OH)_3O^-$. In the aqueous phase, it also includes a Na^+ ion and 64 water molecules. All simulations were performed at a temperature of 350 K with a time step of 0.5 fs.

In the RETIS part, we employed 10 and 15 interfaces for the dissociation and association of silicate complex in the gas phase, and 7 and 15 interfaces for the dissociation of silicate complex and water removal step in aqueous phase, respectively. We used previously computed free energy profiles[16] as a guideline to identify suitable positions of the interfaces. Additionally we used some initial trial simulations to adjust the number of interfaces and their positions. For the water removal step the reaction coordinate is based on the distance between the five-coordinated silicon and hydroxyl oxygen that is released. The first interface, defining the reactant state A, was set at $\lambda_A = 1.85$ Å and the last interface, defining product state B, was set at $\lambda_B = 3.8$ Å. For the cases in which λ_B was crossed without the second reaction step being completed, we used the last configuration and atomistic velocities to start a straightforward molecular trajectory. All of these trajectories showed that the second reaction step followed eventually and none of these trajectories showed the reverse reaction. This implies that crossing λ_B is a valid criterion to assume that basin of attraction of the product state is reached.

At each cycle and each path ensemble, we randomly choose among the different MC moves to be carried out. These are shooting, time-reversal, and replica exchange moves. The selection probability for these moves are equal to 25%, 25%, and 50%, respectively. In total, at least 5000 cycles were performed for the dissociation reaction and 2000 cycles for the association reaction in the gas phase. Each cycle implies an update of each path ensemble with a single Monte Carlo move. In the aqueous phase, we also performed at least 2200 cycles for the dissociation reaction in the aqueous phase and 2500 cycles for the water removal step.

4 Results and Disscusion

For the gas phase we focused on the association and dissociation mechanism, since the water removal step is of little physical relevance in the gas phase. The surrounding hydrogen-bonded network of the aqueous solution is essential element to facilitate the departure of the hydroxyl group. For the aqueous phase, we focused on the dissociation and the water removal step since the height of the association barrier proved to require too much computational resources.

4.1 Gas Phase

Dissociation and association. Here we analyze the first step of this reaction in a small-scale gaseous system in both forward (association) and backward (dissociation). For this purpose, several reactive trajectories along the reaction coordinate were used to investigate the reaction mechanism in the gas phase. Analysis of the reactive molecular dynamics trajectories showed that the dissociation and association reactions occur by the direct mechanism, in which the Si−O bond is dissociated or created without significant disturbance of any of the other molecular bonds (see Figure 3). Figure 3 shows that the silicon atoms and the intermediate oxygen are not exactly aligned, the Si-O-Si angle has a small bend, tilting the oxygen a little upwards (Figure 3). In the dissociation process, the upper hydroxyl groups of the four-coordinated silicate group flip their orientation and make hydrogen bonds

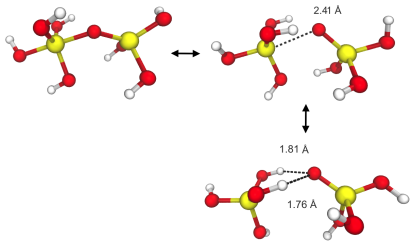

Fig. 3 Representative snapshots of dissociation of silicate complex in gas phase. Distances of Si−O and hydrogen bonds are shown in angstrom (Å)

with the intermediate oxygen. This process is highly symmetric with both hydroxyl groups forming the hydrogen bonds almost simultaneously. However, this process does not lead to a transfer of the proton of any of the hydroxyl groups towards the intermediate oxygen.

Table 1a shows the flux through interface $\lambda_A = 1.95$ Å for dissociation and $\lambda_A = 3.1$ Å for association, the overall crossing probability, and the rate constants which follows as the product of the two for the dissociation and association reactions in gas phase. The rate constant for dissociation is five orders of magnitude higher than the one of the association process. Block analysis indicates statistical errors of 15% and 66% for dissociation and association, respectively.

Figure 4a,b shows the activation energy profiles and the crossing probabilities for association and dissociation calculated from the RETIS path ensembles. The activation energy profile clearly converges to a plateau analogous to the crossing probability. In both panels a, b of Figure 4 we showed the minimized energy previously obtained [16] using DFT geometry optimizations in which the Si-O distance was held fixed at different values ranging from 1.83 til 3.15 Å. This curve corresponds to the so-called zero temperature free energy curve and shows a transition state at 2.38 Å, [16] just before the point were the activation energy curve and the crossing probability starts to become flat. The mismatch in position between the maximum of energy curve obtained from the constrained geometry optimization and the plateau value of the activation energy obtained from RETIS simulation is due to hysteresis [62] caused by the reaction coordinate not being aligned with the eigenvector with negative eigenvalue. The zero temperature free energy barrier for both association and dissociation is close (within 1 kcal/mol) but not identical, which is also logical since they describe related but conceptual different quantities. In our simulations, length of the reactive trajectories ranges between 100 and 400 fs for the dissociation and between 150 and 650 fs for the association process in gas phase.

Table 1 The flux f_A through λ_A, crossing probability $P(\lambda_B|\lambda_A)$, and rate constant k_{AB} for the silicate complex dissociation (Dissoc.), association (Assoc.), and water removal step (Remov.) at 350 K. Results are shown for (a) gas-phase and (b) aqueous phase.

(a) Gas	f_A (s^{-1})	$P(\lambda_B\|\lambda_A)$	k_{AB} (s^{-1})
Dissoc.	6.20×10^{12}	1.24×10^{-2}	7.68×10^{10}
Assoc.	2.23×10^{12}	7.13×10^{-8}	1.59×10^{5}
(b) Aqueous	f_A (s^{-1})	$P(\lambda_B\|\lambda_A)$	k_{AB} (s^{-1})
Dissoc.	6.87×10^{12}	6.92×10^{-5}	4.75×10^{8}
Remov.	8.04×10^{12}	2.53×10^{-6}	2.04×10^{7}

4.2 Aqueous Phase

Dissociation. Figure 4c shows the crossing probability along the reaction coordinate for the dissociation in the aqueous phase. As mentioned above, an accurate evaluation of the activation energy is difficult to obtain for large systems and this was confirmed by our analysis which did not convergence enough to provide a meaningful result. Instead, we show the free energy barrier at 350 K obtained from Ref. 16 as a reference. Table 1b shows the flux through $\lambda_A = 1.85$ Å and overall crossing probability. The rate constants of dissociation in the aqueous phase is about 160 times smaller than in the gas phase implying that the aqueous solution stabilizes the five-coordinated silicate dimer. The length of the reactive trajectories ranged between 0.15 and 4.0 ps.

Representative snapshots for the mechanisms of the dissociation process are shown in Figure 5. The dissociation process can occur through two possible mechanisms which are distinguished from each other by the presence or the absence of an additional proton transfer step. Figure 5a and 5b show two trajectories involving the proton transfer mechanism while Figure 5c shows a reactive trajectory which does not involve a proton transfer. Just like the gas-phase reaction two hydroxyl groups (labeled 1 and 2) at the five-coordinated silicate group tend to point their hydrogens (colored green and purple, respectively) in the direction of the intermediate bridging oxygen. Our path sampling simulations produce reactive transitions which involve either the transfer of hydrogen number 1 (Figure 5a) or number 2 (Figure 5b). The fact that the RETIS simulation manages to produce both types of trajectories provides confidence that the sampling is ergodic. Although the orientation of the hydroxyl groups look initially symmetric, just like the gas-phase reaction, the symmetry is sometimes broken by the solvent structure which seems to catalyze the proton transfer step. Figure 5a and 5b show the presence of water molecule (with its oxygen colored orange) forming a hydrogen bond with the bridging oxygen atom. The hydrogen bond creates a pulling force on the bridging oxygen which brings the oxygen closer towards one of the hydroxyl groups 1 or 2 which enables the proton transfer at the point where the silicon-oxygen bond breaks. In the reactive trajectories where the hydrogen bond is absent no proton transfer was observed (like in Figure 5c) similar to the gas phase reaction. In all cases where the bridging oxygen accepted a hydrogen bond from the solvent, the proton transfer from one of the two hydroxyl groups always occurred at the side of the water molecule donating the bond. Although both mechanisms contribute to the dissociation of the silicate complex, our results infer that the mechanism with proton transfer is predominant with a probability of about 80% compared to the mechanism without proton transfer.

Removal of water. The energy barrier for water removal step is higher than dissociation process. [10,11,13] Free energy for the water removal step in the silicate dimerization has a maximum at

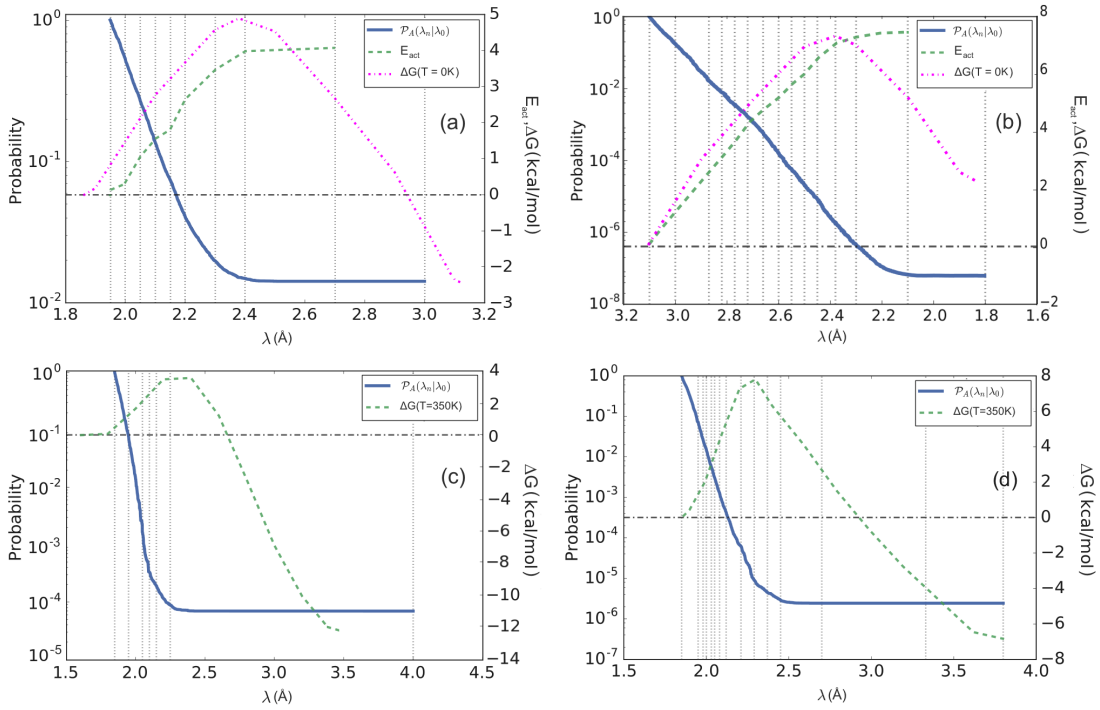

Fig. 4 Crossing probabilities as function of RC for the silicate condensation at 350 K. The positions of the interfaces are indicated with vertical dashed lines. (a) Dissociation reaction of silicate complex, (b) Association reaction of silicate complex in gas phase. The DFT free energy profile was calculated at 0 K using the BLYP functional including Grimme dispersion correction[63] and the QZ4P[64] basis set.[16] (c) Dissociation reaction of silicate complex in aqueous phase. The free energy profile was calculated from constrained molecular dynamics simulation using the BLYP functional and the DZVP-MOLOPT basis set.[16] (d) Water removal step, free energy profile obtained from Ref. 13.

silicon-oxygen distance 2.4 Å.[13] Figure 4d illustrates the overall crossing probability as function of reaction coordinate for the water removal step. It clearly shows a plateau at 2.4 Å, indicating that the barrier of water removal step has been crossed. The flux and overall crossing probability are shown in Table 1b. The rate constant for the water removal step is almost one order of magnitude less than dissociation process and is about $2.04\times10^{7}\ s^{-1}$. The length of trajectories ranges from 0.06 to 40 ps depending on the mechanism and number of water molecules involved in the proton transfer process.

During the water removal process, one hydroxyl group leaves the five-coordinated silicon, remains in the solution for a while, and then receives a proton, neutralizing the OH^- ion. The last step can either occur directly via the silicate complex (internal) or by means of the solvent via a hydrogen bond network (external). The internal proton transfer mechanism implies that the leaving OH group receives a proton directly via a deprotonation of a Si−OH group, while in the external proton transfer, one or several water molecules transfer their proton through a hydrogen bond wire via a Grotthuss mechanism.[65] This process ends when the Si−OH group releases a proton neutralizing the OH^- ion. Hence, in both cases the reaction ends after the deprotonation of a Si−OH group generating the anionic silicate dimer $H_5Si_2O_7^-$ (see Figure 6).

Despite that the reaction coordinate is flexible, not specifying which hydroxyl group at the five-coordinated silicon should release (see Figure 2b), our simulation showed that the leaving OH group is always the group most distant from the other silicon (with its oxygen colored green in Figure 6). In addition, the simulations reveal that both internal and external mechanisms contribute to the overall reaction, though the internal proton transfer is favored and happens in 58% of the occasions. Previous studies suggested that the hydroxyl release step occurs simultaneously with the deprotonation of the Si−OH group.[10,11,13] However, our study indicates that the OH group remains in the solution 0.06−3.5 ps in the internal mechanism and 0.1−40 ps in the external mechanism before it neutralizes. Hence, the reaction forming the anionic silicate dimer $H_5Si_2O_7^-$ is step-wise and not concerted. This illustrates the advantage of the RETIS approach compared to constrained MD. In the constrained MD simulations, the release of the OH group occurs more gradually since at each increment of the reaction coordinate its value is fixed for a while and the system is given time to adapt to the new situation. In the unbiased MD trajectories harvested by the RETIS algorithm, there is no adaptation time and the hydroxyl can escape into the solvent without giving a chance to the rest of the silicate complex to release its proton. Hence, RETIS is able to disclose a more realistic dynamical evolution of a complex process. Though, it should be realized that also these results do not describe the exact physical behavior as our simulations are affected as well by the choice of functional, finite size effects of the simulation box, and the purely classical description of the protons. A further de-

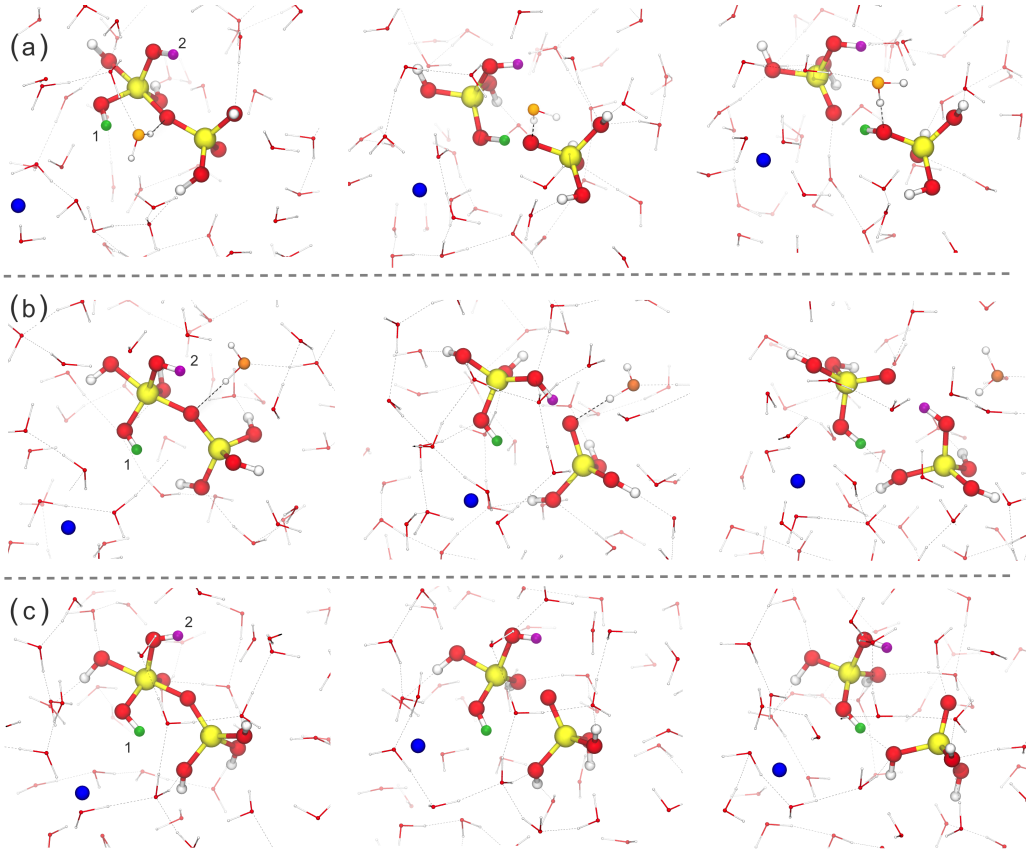

Fig. 5 Representative snapshots of different dissociation mechanism of silicate complex in aqueous phase. Hydrogens with possibility of involving in the dissociation process are shown in green and purple colors. Water molecule with hydrogen bond to the bridging oxygen is shown in orange and Na^+ ion is colored in blue. (a), (b) Mechanism with hydrogen transfer (c) Mechanism without hydrogen transfer.

velopment of experimental techniques to measure signatures of these type of reaction mechanism would, therefore, be very useful to benchmark these type of rare event simulations.

Figure 6 shows the selected snapshots for initial stages of water removal process. In most cases, as shown in Figure 6a and 6b, one of Si−OH groups (oxygen colored in brown) on the five-coordinated silicon is pointing towards the leaving OH group, acting as a proton donor to the hydroxide via an internal proton transfer. Also for the cases in which the proton transfers externally, i.e. via the solvent, it is this hydroxyl group that most often releases its proton. However, if the release of the OH group is not rapidly follow-up by the proton release, also the other hydroxyl groups may act as proton donor (as in Figure 6b). In 24% of the cases of the external proton transfer a Si−OH group from the four-coordinate silicon acts as proton donor. This can occur when the hydroxide ion has sufficient time to effectively diffuse (via the Grotthuss mechanism) towards the four-coordinated silicon. In some but not all cases this happens via the periodic boundaries. Figure 7 shows the time distribution of the reactive trajectories indicating the time interval between OH release and silicate deprotonation for both internal and external mechanism. Clearly, the average trajectory length of the external mechanism is considerably longer than that of the internal mechanism. This is a result of the external mechanism consisting of several proton transfer reaction steps.

However, as can be seen from Figure 7a, also the internal mechanism has a relatively broad double peaked distribution. This is because also in the internal mechanism solvent molecules can participate in intermediate reaction steps. The released OH group then receives a proton from the solvent but eventually gives it back and finally accepts a proton from the silicate complex. We observed that there can be a maximum of two water molecules involved in these temporary proton excursions as shown in the inset of Figure 7a. The double peaked distribution is a direct result of having either zero or one solvent molecule or two molecules involved.

In the external mechanism, the proton transfer occurs along a hydrogen bond wire. Water molecules in solution construct a hydrogen bonds network that facilitates the water removal step. The inset of Figure 7b shows the number of water molecules involved in the hydrogen wire before neutralization occurs via the deprotonation of the silicate. In some cases, the proton transfer from a solvent molecule towards the hydroxide jumps back after a very short time. These water molecules were not counted as being part of the hydrogen bond wire. The silicon deprotonation seems irreversible which is in contrast to what constraint molecular dynamics suggest.[13]

Figure 6c shows a non-reactive trajectory in the water removal

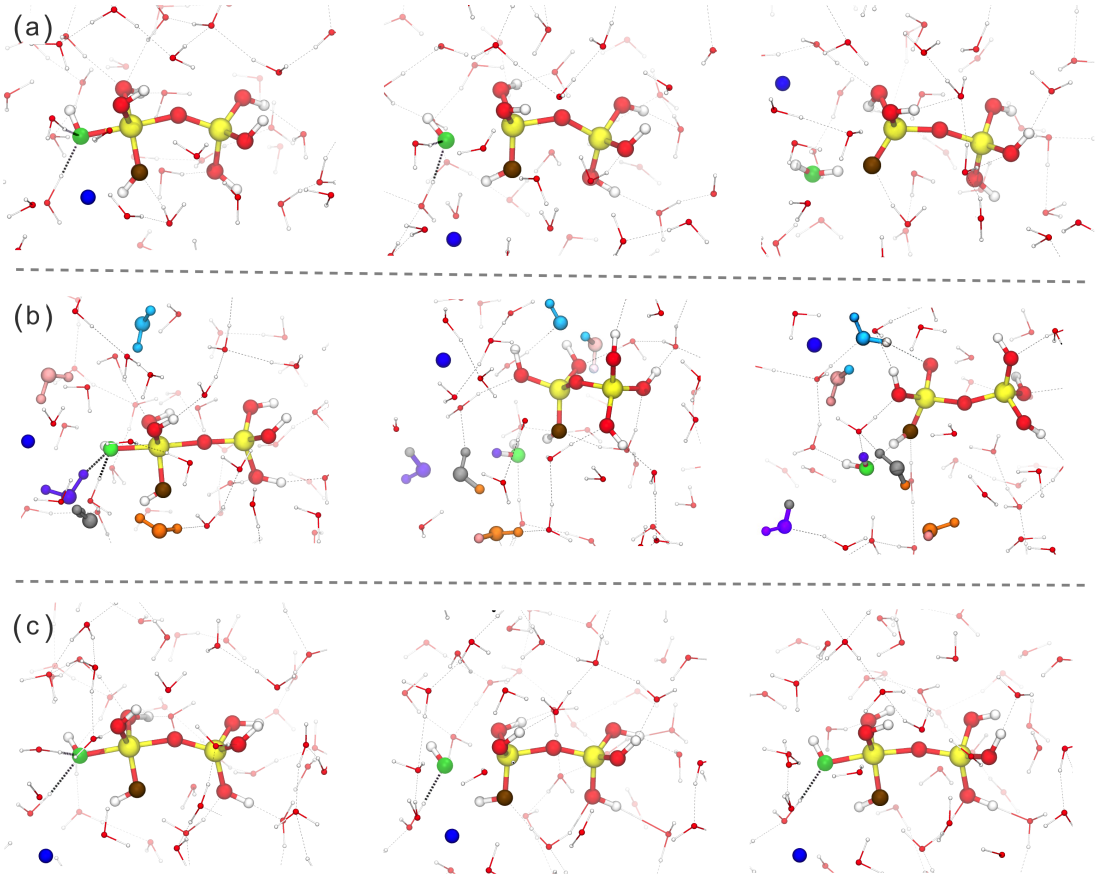

Fig. 6 Representative snapshots of water removal step in the silicate condensation process. The oxygen of leaving OH group and Na^+ ion are shown in green and blue colors respectively. (a) Internal mechanism: Proton transfers directly from the deprotonation of a Si−OH group (b) External mechanism: Proton transfer occurs through the Grotthuss mechanism. Water molecules involved in the hydrogen bonds network are shown bold and different colors, (c) Non-reactive trajectory and effect of the presence and absence of hydrogen bonds on the leaving OH group in the water removal step. In the first frame of the three trajectories always one hydroxyl group is pointed towards the leaving OH group (colored brown). It is this hydroxyl group that always gets deprotonated in the internal mechanism and most often in the external mechanism as well (but not for trajectory (b)). Having at least two hydrogen bonds between the leaving OH group and the solvent seems a prerequisite for the reaction to succeed. The second frame of trajectory (c) shows that only one hydrogen bond remained after the initial release and since the OH group is still in the vicinity of the silicate complex the five-coordinated silicate complex is quickly reformed.

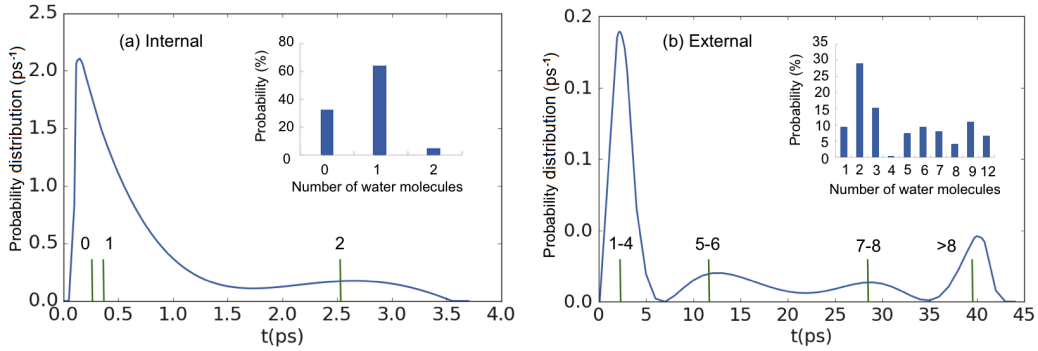

Fig. 7 Time distribution of the reactive trajectories indicating the time interval between OH group release and silicate deprotonation for (a) internal mechanism and (b) external mechanism. The inset (a) shows number of water molecules involved in temporary proton excursions in the internal mechanism. The inset (b) shows number of water molecules involved in the hydrogen wire in the external mechanism of water removal step. Vertical lines show the average trajectory length with respect to the number of water molecules involved in the hydrogen bond wire.

step. We observed that at least two hydrogen bonds are required to pull and dissociate the OH group from the five-coordinate silicon. These hydrogen bonds are essential to depart the hydroxyl group from silicate in opposite directions and to avoid the recom-

bination process. After that the hydroxide ion can participate in the Grotthuss mechanism and becomes neutralized.

5 Conclusions

In this paper, we have performed a path sampling simulation based on the RETIS algorithm in combination with Ab Initio molecular dynamics to investigate the mechanisms and the rate of silicate dimerization reactions in gas and aqueous phase. For this purpose, we generated in total around one hundred thousand trajectories. Regarding force evaluations, each reaction study in the aqueous phase corresponded to ca. 1000-1400 ps. Still, by means of the RETIS rare event approach, we obtain inverse rate constants (the expectation time of the chemical event) as high as 50 000 ps and a couple of thousands reactive trajectories. In other words, the RETIS simulations provide results which would otherwise require a 100 μs brute force molecular dynamics simulation which is far beyond reach for Ab Initio molecular dynamics.

RETIS simulations show that the rates of SiO−Si bond dissociation in the aqueous phase is reduced by a factor of about 160, compared to the gas phase results. This implies that the aqueous solution stabilizes the five-coordinated silicate dimer. Interestingly, the dissociation of silicate complex in the aqueous phase may either occur via a proton assisted mechanism or via a mechanism without proton transfer. We highlighted the role and importance of water molecule arrangement in the dissociation mechanism. A water molecule forms a hydrogen bond with the bridging oxygen atom in silicate complex and causes a pulling force on the oxygen towards one of the hydroxyl groups and enables the proton transfer at the silicon-oxygen bond breakage point. The mechanism with proton transfer is highly predominant compared to the mechanism without proton transfer.

Also the water removal step may occur through two possible mechanisms, the internal and external mechanism, which are distinguished by the proton transfer reaction path. This implies that proton transfer can either occur via a direct or via a water mediated reaction step. In the internal proton transfer mechanism the leaving hydroxyl group accepts a proton directly via a silicate deprotonation step, while in the external proton transfer, one or several water molecules transfer their protons through a hydrogen bond wire via a Grotthuss mechanism. Previous studies have provided contradicting conclusions regarding the role of solvent in the water removal step in the silicate dimerization reaction as some have reported that it occurs solely via the internal mechanism[10] while other studies suggest it occurs via the external mechanism.[13] More recently, McIntosh[11] observed both mechanisms, but claimed that it is unlikely that the external proton transfer is competitive with the direct proton transfer. In contrast, the unbiased dynamical trajectories generated by the RETIS simulation show that both mechanisms can occur and the internal mechanism only is slightly favorable compared to the external mechanism. The length of these trajectories highly depend on the mechanisms and number of water molecules involved in the hydrogen bonds wire. The presence of hydrogen bonds between the leaving hydroxyl group and the solvent acts as a prerequisite for the reaction to succeed.

In summary, RETIS allowed the calculation of rate constants as well as to give valuable insight into which reaction mechanism dominates when dynamics and explicit solvent are taken into account. We believe that the technique presented here can open many possible avenues in the field of silicate oligomerization reactions and chemical reactions in general. Besides the fundamental new insight, these type of simulations will eventually help to obtain a better control of chemical reactions and provide new inspiration for alternative synthesis methods and the creation of other silicate materials.

Acknowledgments

The authors thank the Research Council of Norway project no. 237423 and the Faculty of Natural Sciences and Technology (NTNU) for support. Computational resources were granted by The Norwegian Metacenter for Computational Science (NOTUR), project NN9254K.

References

1 P. E. A. de Moor, T. P. M. Beelen, R. A. van Santen, K. Tsuji, and M. E. Davis. SAXS and USAXS investigation on nanometer-scaled precursors in organic-mediated zeolite crystallization from gelating systems. *Chem. Mater.*, 11:36–43, 1999.

2 P. E. A. de Moor, T. P. M. Beelen, R. A. van Santen, L. W. Beck, and M. E. Davis. Si-mfi crystallization using a DimerĂİ and Trimer of tpa studied with small-angle x-ray scattering. *J. Phys. Chem. B*, 104:7600–7611, 2000.

3 A. R. Felmy, H. Cho, James R. Rustad, and M. J. Mason. An aqueous thermodynamic model for polymerized silica species to high ionic strength. *J. Solution Chem.*, 30:509–525, 2001.

4 J. M. Fedeyko, D. G. Vlachos, and R. F. Lobo. Formation and structure of self-assembled silica nanoparticles in basic solutions of organic and inorganic cations. *Langmuir*, 21:5197–5206, 2005.

5 S. A. Pelster, W. Schrader, and F. Schüth. Monitoring temporal evolution of silicate species during hydrolysis and condensation of silicates using mass spectrometry. *J. Am. Chem. Soc.*, 128:4310–4317, 2006.

6 J. C. G. Pereira, C. R. A. Catlow, and G. D. Price. Silica condensation reaction: an ab initio study. *Chem. Commun.*, 115:1387–1388, 1998.

7 J. C. G. Pereira, C. R. A. Catlow, and G. D. Price. Ab initio studies of silica-based clusters. part I. energies and conformations of simple clusters. *J. Phys. Chem. A*, 103:3252–3267, 1999.

8 J. C. G. Pereira, C. R. A. Catlow, and G. D. Price. Ab initio studies of silica-based clusters. part II. structures and energies of complex clusters. *J. Phys. Chem. A*, 103:3268–3284, 1999.

9 M. J. Mora-Fonz, C. R. A. Catlow, and D. W. Lewis. Oligomerization and cyclization processes in the nucleation of microporous silicas. *Angew. Chem. Int. Ed.*, 44:3082–3086, 2005.

10 T. T. Trinh, A. P. J. Jansen, R. A. van Santen, and E. Jan Meijer. The role of water in silicate oligomerization reaction. *Phys. Chem. Chem. Phys.*, 11:5092–5099, 2009.

11 G. J. McIntosh. A theoretical kinetic model of the temperature

and ph dependent dimerization of orthosilicic acid in aqueous solution. *Phys. Chem. Chem. Phys.*, 14:996–1013, 2012.

12 T. T. Trinh, X. Rozanska, F. Delbecq, and P. Sautet. The initial step of silicate versus aluminosilicate formation in zeolite synthesis: a reaction mechanism in water with a tetrapropylammonium template. *Phys. Chem. Chem. Phys.*, 14:3369–3380, 2012.

13 A. Pavlova, T. T. Trinh, R. A. van Santen, and E. J. Meijer. Clarifying the role of sodium in the silica oligomerization reaction. *Phys. Chem. Chem. Phys.*, 15:1123–1129, 2013.

14 G. J. McIntosh. Theoretical investigations into the nucleation of silica growth in basic solution part II derivation and benchmarking of a first principles kinetic model of solution chemistry. *Phys. Chem. Chem. Phys.*, 15:17496–17509, 2013.

15 G. J. McIntosh. Theoretical investigations into the nucleation of silica growth in basic solution part I ab initio studies of the formation of trimers and tetramers. *Phys. Chem. Chem. Phys.*, 15:3155–3172, 2013.

16 M. Moqadam, E. Riccardi, T. T. Trinh, P.-O. Åstrand, and T. S. van Erp. A test on reactive force fields for the study of silica dimerization reactions. *J. Chem. Phys.*, 143:184113–8, 2015.

17 H. Henschel, A. M. Schneider, and M. H. Prosenc. Initial steps of the Sol-Gel process: Modeling silicate condensation in basic medium. *Chem. Mater.*, 22:5105–5111, 2010.

18 J.A. Tossell. Theoretical study on the dimerization of $Si(OH)_4$ in aqueous solution and its dependence on temperature and dielectric constant. *Geochim. Cosmochim. Acta*, 69:283–291, 2005.

19 Y. T. Xiao and A. C. Lasaga. Ab initio quantum mechanical studies of the kinetics and mechanisms of quartz dissolution: OH-catalysis. *Geochim. Cosmochim. Acta*, 60:2283–2295, 1996.

20 H. Hu, H. Hou, Z. He, and B. Wang. Theoretical characterizations of the mechanism for the dimerization of monosilicic acid in basic solution. *Phys. Chem. Chem. Phys.*, 15:15027–15032, 2013.

21 T. T. Trinh, A. P. J. Jansen, R. A. van Santen, and E. J. Meijer. Role of water in silica oligomerization. *J. Phys. Chem. C*, 113:2647–2652, 2009.

22 T. T. Trinh, A. P. J. Jansen, and R. A. Santen. Mechanism of oligomerization reactions of silica. *J. Phys. Chem. B*, 110:23099–23106, 2006.

23 T. T. Trinh, A. P. Jansen, R. A. van Santen, J. VandeVondele, and E. J. Meijer. Effect of counter ions on the silica oligomerization reaction. *Comput. Phys. Commun.*, 10:1775–1782, 2009.

24 E. A. Carter, G. Ciccotti, J. T. Hynes, and R. Kapral. Constrained reaction coordinate dynamics for the simulation of rare events. *Chem. Phys. Lett.*, 156:472, 1989.

25 J. Tersoff. New empirical model for the structural properties of silicon. *Phys. Rev. Lett.*, 56:632–635, 1986.

26 F. H. Stillinger and T. A. Weber. Computer simulation of local order in condensed phases of silicon. *Phys. Rev. B*, 31:5262–5271, 1985. Erratum in 33, 1451, 1986.

27 F. H. Stillinger and T. A. Weber. Fluorination of the dimerized Si(100) surface studied by molecular-dynamics simulation. *Phys. Rev. Lett.*, 62:2144–2147, 1989.

28 D. Kohen, J. C. Tully, and F. H. Stillinger. Modeling the interaction of hydrogen with silicon surfaces. *Surf. Sci.*, 397:225–236, 1998.

29 A. Ostadhossein, E. D. Cubuk, G. A. Tritsaris, E. Kaxiras, S. Zhang, and A. C. T. van Duin. Stress effects on the initial lithiation of crystalline silicon nanowires: reactive molecular dynamics simulations using ReaxFF. *Phys. Chem. Chem. Phys.*, 17:3832–3840, 2015.

30 A. C. T. van Duin, S.h Dasgupta, F. Lorant, and W. A. Goddard. ReaxFF: A reactive force field for hydrocarbons. *J. Phys. Chem. A*, 105:9396–9409, 2001.

31 S. Agrawalla and A. C. T. van Duin. Development and application of a ReaxFF reactive force field for hydrogen combustion. *J. Phys. Chem. A*, 115:960–972, 2011.

32 A. C. T. van Duin, A. Strachan, S. Stewman, Q. Zhang, X. Xu, and W. A Goddard. $ReaxFF_{SiO}$ reactive force field for silicon and silicon oxide systems. *J. Phys. Chem. A*, 107:3803–3811, 2003.

33 W. M. Young and E. W. Elcock. Monte carlo studies of vacancy migration in binary ordered alloys: I. *Proc. Phys. Soc. London*, 89:735, 1966.

34 X. Zhang, T. T. Trinh, R. A. van Santen, and A. P. J. Jansen. Structure-directing role of counterions in the initial stage of zeolite synthesis. *J. Phys. Chem. C*, 115:9561–9567, 2011.

35 X. Zhang, T. T. Trinh, R. A. van Santen, and A. P. J. Jansen. Mechanism of the initial stage of silicate oligomerization. *J. Am. Chem. Soc.*, 133:6613–6625, 2011.

36 M. Ciantar, C. Mellot-Draznieks, and C. Nieto-Draghi. A kinetic monte carlo simulation study of synthesis variables and diffusion coefficients in early stages of silicate oligomerization. *J. Phys. Chem. C*, 119:28871–28884, 2015.

37 J. C. Fogarty, H. M. Aktulga, A. Y. Grama, A. C. T. Van Duin, and S. A Pandit. A reactive molecular dynamics simulation of the silica-water interface. *J. Chem. Phys.*, 132:174704–174710, 2010.

38 H. R. Larsson, A. C. T. van Duin, and B. Hartke. Global optimization of parameters in the reactive force field ReaxFF for SiOH. *J. Comput. Chem.*, 34:2178–2189, 2013.

39 C. Dellago, P. G. Bolhuis, F. S. Csajka, and D. Chandler. Transition path sampling and the calculation of rate constants. *J. Chem. Phys.*, 108:1964–1977, 1998.

40 T. S. van Erp, D. Moroni, and P. G. Bolhuis. A novel path sampling method for the calculation of rate constants. *J. Chem. Phys.*, 98:7762–7774, 2003.

41 T. S. van Erp. Reaction rate calculation by parallel path swapping. *Phys. Rev. Lett.*, 98:268301, 2007.

42 P. L. Geissler, C. Dellago, D. Chandler, J. Hutter, and M. Parrinello. Autoionization in liquid water. *Science*, 291:2121–2124, 2001.

43 B. Ensing, , and E. Jan Baerends. Reaction path sampling of the reaction between iron(II) and hydrogen peroxide in

aqueous solution. *J. Phys. Chem. A*, 106:7902–7910, 2002.

44 G. Reinisch, J. Leyssale, and G. L. Vignoles. Theoretical study of the decomposition of BCl_3 induced by a h radical. *J. Phys. Chem. A*, 115:4786–4797, 2011.

45 Z. Wang, D. Antoniou, S. D. Schwartz, and V. L. Schramm. Hydride transfer in DHFR by transition path sampling, kinetic isotope effects, and heavy enzyme studies. *Biochemistry*, 55:157–166, 2016.

46 R. Car and M. Parrinello. Unified approach for molecular dynamics and density-functional theory. *Phys. Rev. Lett.*, 55:2471–2474, 1985.

47 Cp2k: High performance computing, http://www.nanosim.mat.ethz.ch/research/CP2K.

48 T. Dauxois, M. Peyrard, and A. R. Bishop. Entropy-driven dna denaturation. *Phys. Rev. E*, 47:R44–R47, 1993.

49 C. Dellago, P. G. Bolhuis, and D. Chandler. Efficient transition path sampling: Application to lennard-jones cluster rearrangements. *J. Chem. Phys.*, 108:9236–9245, 1998.

50 Ti. S. van Erp and P. G. Bolhuis. Elaborating transition interface sampling methods. *J. Comp. Phys.*, 205:157–181, 2005.

51 C. Dellago and P. G. Bolhuis. Activation energies from transition path sampling simulations. *Mol Simul*, 30:795–799, 2004.

52 J. VandeVondele, M. Krack, F. Mohamed, M. Parrinello, T. Chassaing, and J. Hutter. Quickstep: Fast and accurate density functional calculations using a mixed gaussian and plane waves approach. *Comput. Phys. Commun.*, 167:103–128, 2005.

53 A. D. Becke. Density-functional exchange-energy approximation with correct asymptotic behavior. *Phys. Rev. A*, 38:3098–3100, 1988.

54 C. Lee, W. Yang, and R. G. Parr. Development of the colle-salvetti correlation-energy formula into a functional of the electron density. *Phys. Rev. B*, 37:785–789, 1988.

55 J. Andzelm J. Baker, M. Muir and A. Scheiner. Hybrid hartree-fock density-functional theory functionals: The adiabatic connection method. *ACS Symposium Series*, 629:342–367, 1996.

56 S. Grimme. Semiempirical GGA-type density functional constructed with a long-range dispersion correction. *J. Comput. Chem.*, 27:1787–1799, 2006.

57 S. Goedecker, M. Teter, and J. Hutter. Separable dual-space gaussian pseudopotentials. *Phys. Rev. B*, 54:1703–1710, 1996.

58 C. Hartwigsen, S. Goedecker, and J. Hutter. Relativistic separable dual-space gaussian pseudopotentials from H to Rn. *Phys. Rev. B*, 58:3641–3662, 1998.

59 M. Sprik, J. Hutter, and M. Parrinello. Ab initio molecular dynamics simulation of liquid water: Comparison of three gradient-corrected density functionals. *J. Chem. Phys.*, 105:1142–1152, 1996.

60 C. Mischler, J. Horbach, W. Kob, and K. Binder. Water adsorption on amorphous silica surfaces: a car-ĂŞparrinello simulation study. *J. Phys.: Condens. Matter*, 17:4005–4013, 2005.

61 J. VandeVondele and J Hutter. Gaussian basis sets for accurate calculations on molecular systems in gas and condensed phases. *J. Chem. Phys.*, 127:114105–114105, 2007.

62 T. S. van Erp and E. J. Meijer. Proton assisted ethylene hydration in aqueous solution. *Angew. Chemie*, 43:1659–1662, 2004.

63 S. Grimme, S. Ehrlich, and L. Goerigk. Effect of the damping function in dispersion corrected density functional theory. *J. Comput. Chem.*, 32:1456–1465, 2011.

64 G. Maroulis. *Computational Aspects of Electric Polarizability Calculations: Atoms, Molecules and Clusters*. IOS Press, Amsterdam, 2006.

65 C. J. T. de Grotthuss. Memoir on the decomposition of water and of the bodies that it holds in solution by means of galvanic electricity. *Biochimica et Biophysica Acta*, 1757:871–875, 2006.